

We are IntechOpen, the world's leading publisher of Open Access books Built by scientists, for scientists

6,900

Open access books available

186,000

International authors and editors

200M

Downloads

Our authors are among the

154

Countries delivered to

TOP 1%

most cited scientists

12.2%

Contributors from top 500 universities



WEB OF SCIENCE™

Selection of our books indexed in the Book Citation Index
in Web of Science™ Core Collection (BKCI)

Interested in publishing with us?
Contact book.department@intechopen.com

Numbers displayed above are based on latest data collected.
For more information visit www.intechopen.com



Artifacts in Atomic Force Microscopy of Biological Samples

E. Ukraintsev, A. Kromka, H. Kozak, Z. Remeš and B. Rezek
*Institute of Physics, Academy of Sciences of the Czech Republic, Prague 6
 Czech Republic*

1. Introduction

Atomic force microscopy (AFM) is a frequently used method applicable also to biological studies due to its capability of measuring in native environment. Sharp Si, Si₃N₄ or C (carbon nanotubes, diamond, diamond coated) cantilevers repeatedly touching a sample are used in this method as sensitive probes. It is possible to control the interaction between the tip and the sample in order to make less invasive measurements or, conversely, to modify the sample. However, AFM images often contain features which are not present on the sample in reality, but are a direct result of the measurements itself. Such structures or features are denoted as artifacts. The artifacts arise from various reasons. Some of them can be avoided during measurements, other ones are inherent. The artifacts shown in this chapter are divided into several categories based on the part of AFM which is responsible for them. Examples of many artifacts are presented and their reasons are explained. This chapter will be helpful for AFM users who observe strange effects, presumably related to the AFM technique, but do not know their reason. This chapter can also answer questions about the validity of imaged features as well as their accuracy.

AFM is commonly used in biology to study proteins (Ukraintsev et al., 2007; Ukraintsev et al., 2009; Rezek et al., 2009), peptides (Kransnoslobodtsev et al., 2005), DNA (Hamon et al., 2007), tissues (Graham et al., 2010), viruses (Kuznetsov et al., 2003) and living cells (H. X. You & Yu, 1999). The possibility to perform such measurements *in situ* is the main advantage of this technique. On the other hand, optical and electron microscopy are not so often used for environmental examination in biology. More specifically, optical and fluorescence microscopy are usually applied on stained cells because non-stained cells are practically transparent. Scanning electron microscope (SEM) measurements are usually performed on dried samples with a few exceptions employing environmental SEM (Hawkes, 1988). Another important factor is high spatial resolution; for example, AFM can resolve individual spread molecules of ssDNA (Klinov et al., 2009) or even the morphology of upright dsDNA molecules (Rezek et al., 2006; Rezek, Shin & Nebel, 2007).

In situ studies of soft matter in a solution can reveal different protein conformations, which are not detectable in air (Moreno-Herrero et al., 2004; Rezek et al. 2009, Rezek et al., 2011). Besides, cell morphology in an air and in a medium is different. However, AFM imaging in solution can be difficult since the tip-molecule interaction must be tuned to be weaker than the molecule-substrate interaction. Van der Waals forces are screened off in liquids, making

molecule-substrate interaction weak. For this reason, the AFM imaging technique must be chosen in a way which minimizes intrusiveness (Moreno-Herrero et al., 2004).

Using AFM, one can *in situ* study not only cell morphology (H. X. You & Yu, 1999), but also mechanical properties of an individual cell (Müller et al., 2009). For cells attached to a sample, the force scanning method produces high-resolution spatial modulus map (Darling, 2011) and force spectroscopy reveals elastic and adhesive properties of cell membranes (Volle et al., 2008; Kwon et al., 2009). For cells attached to a cantilever, the force spectroscopy method gives information about the interaction between cells and diamond surfaces with different chemistry (Chong et al., 2007; Helenius et al., 2008).

However, AFM has some disadvantages. First of all, it is an invasive method (H. X. You & Yu, 1999) with a few exceptions like non-contact mode measurements in vacuum (Maeda et al., 1999) and in solution (Checco et al., 2006). Usually, the influence is undesirable, but in some cases it has potential. For example, AFM tip can be used as a “nanoscalpel” or “nanoneedle” for surgery of biological cells (Beard, Gordeev & Guy, 2011) or as a spade to remove proteins from the surface (Rezek et al., 2009). Second, it is a slow method. Nevertheless, it is possible to measure much faster using either a small cantilever (Crampton et al., 2007), spiral scanning (Mahmood & Moheimani, 2009) or contact mode (CM) with controllable force (Choi et al., 2008). Third, an AFM image does not always correspond to real morphology (Ricci & Braga, 2003; Su, Wei & Liu, 2005; Eaton, 2010). One can even postulate that the real morphology always differs from the shape measured by AFM.

AFM is a commonly used technique with applications in different fields; however, only a limited number of articles has been published about AFM artifacts (Kühle et al., 1998; Ricci & Braga, 2003; Velegol et al., 2003; Eaton, 2010; Rezek, Ukraintsev & Kromka, 2011). A number of artifacts related to the study of cells were analyzed and the influence of different AFM parameters (scanning mode, tip shape) on measured parameters (cellular volume, particles height) were discussed (Wu et al., 2008). Artificially formed features can be divided into four categories: artifacts related to the tip, to the scanner, to the sample and artifacts related to the interaction between them.

For example, an artifact related to the tip is the so-called double tip (Y. Chen et al., 2004). A finite tip radius and a pyramidal tip shape causes broadening of the image (Klinov et al., 2009) and shadows around high objects, respectively (Velegol et al., 2003). Piezoelectric creep, thermal drift and scanner-induced vibrations are the main problems associated with the scanner. They can cause the distortion of the image and additional noise (Mahmood & Moheimani, 2009). The sample can be too sticky or too soft. In this case, artifacts due to multiple probe-sample contact points occur (Morton et al., 2003; Sokolov, 2007). AFM image of a charged nonconductive sample may not correspond to topography. Charge distribution measured by AFM may not fully correspond to the real charge distribution (Lambert, Guthmann & Saint-Jean, 2003). A “contrast reversal” artifact is an effect which causes wrong height determination. It is related to the tip-sample interaction and to the switching between attractive and repulsive regimes (Kühle et al., 1998).

Sometimes researchers publish articles about new effects and others claim that the observed effects are due to AFM-related artifacts. For example, Azulay and coworkers presented the “comprehensive local probe study”, which, from their point of view, “clearly indicates that the dominant transport route in undoped $\mu\text{c-Si:H}$ is in the disordered tissue that

encapsulates the crystallites columns" (Azulay et al., 2005). But Vetushka and coworkers state "a completely different origin of the higher conductivity at the grain boundaries, namely, the influence of surface oxidation induced by the tip when the sample is positively biased" (Vetushka et al., 2010), i.e. they claim that the observed effect is due to local anodic oxidation, an artifact of Kelvin force microscopy. Another example is the work of Sajanlal and Pradeep, who presented the formation of well-aligned gold nanotriangle arrays on indium tin oxide substrate (Sajanlal & Pradeep, 2008), but Diao with coworkers state that those triangles are tip artifacts (Diao et al., 2009). The purpose of this chapter is to show different AFM artifacts relevant to biological specimens, explain their reasons and present a way to avoid them.

2. Materials and methods

In this section our biological specimens as well as measurement methods are described. As our substrate of choice for biological studies, we use the monocrystalline diamond (MCD) as it is a well-defined and chemically tailorable substrate (Rezek et al., 2007; Rezek et al., 2010).

Bulk MCD was prepared by chemical vapor deposition and chemically cleaned in acids (97.5 % H_2SO_4 + 99 % powder KNO_3) at 200 °C for 30 minutes. The surface was then hydrogenated at 800 °C for 10 minutes. The MCD substrates were lithographically processed to generate alternating H- and O-terminated patterns of 30 μm widths. A positive photoresist ma-P 1215 (micro resist technology GmbH, Germany) was applied. The MCD substrates with lithography mask were treated in oxygen radio-frequency plasma (300W power, 1 minute process time) to oxidize the surface and hence to generate hydrophilic patterns. Then the sample was rinsed in acetone, photoresist stripper, de-ionized water and dried by air blow. This process minimized possible surface contamination (Rezek & Nebel, 2006). The H-/O-termination quality was proved by a scanning electron microscope (SEM; JEOL Superprobe 733). Electronic measurements detected a surface conductivity of 10^{-5} S/sq on the H-terminated surfaces (Kozak et al., 2009). Surfaces with O-termination were highly resistive. The H-terminated diamond is a hydrophobic surface, contact angle ~ 80 -100 °. The O-terminated diamond has hydrophilic properties, contact angle ~ 5 -20 °.

Proteins were adsorbed on the MCD substrates from 15 % fetal bovine serum (FBS) solution (PAA) in McCoy's 5A medium with stable Glutamine without Phenolred (BioConcept). The serum contains several proteins, usually bovine serum albumin, fibronectin and vitronectin. FBS is heat inactivated (56 °C, 25 min) to destroy the immunological components yet to preserve the proteins. 1 ml of this solution was applied on a diamond surface and in-situ measurements were performed. All experiments were performed at room temperature.

As a common bio-linker, an organosilane layer containing amino-groups ($-\text{NH}_2$) was adsorbed on the O-terminated MCD substrate from an organosilane coupling agent N-(6-aminohexyl) aminopropyl trimethoxysilane (AHAPS, purchased in liquid form from Gelest Ltd., UK). The O-terminated MCD substrate was placed into a quartz cuvette filled with AHAPS solution diluted with absolute toluene and left in dark (chemical method) or exposed to UV irradiation (photochemical method) (Kozak et al., 2011). Both methods of MCD amination were performed for 3 hours at room temperature.

AFM devices from diverse manufactures were used for the study of proteins and the AHAPS layers on the diamond substrates. NTEGRA (NT-MDT) and Dimension (Veeco) AFMs were used, both in tapping mode (TM) and CM as well as in air and in solution. Different types of cantilevers were used, ranging from very soft ($k = 0.06$ N/m) to very stiff ($k = 120$ N/m). Ordinary cantilevers with tips $r \sim 10$ nm (Multi75Al, NSG, CSG) and ultrasharp tips (NTI Europe) were employed.

A critical parameter for any AFM measurement is a set point. The set point value (SP) is the ratio between the amplitude of oscillation during scanning A and the free oscillation amplitude near the surface A_0 . Let us define also SP_0 value as a maximal value of SP which can be used to observe a normal (“true”) image. If $SP > SP_0$, cantilever will lose contact. The SP value for noninvasive measurements should be slightly lower than SP_0 . If $SP \ll SP_0$ and $SP \sim 0$, the force applied to the tip makes this TM similar to CM in terms of applied force. Set point ratio of $SP \sim 0.5$ - 0.7 was used for most of the images unless specified otherwise. Usually, for studies in solution, the SP_0 value for Multi75Al tip is around $SP_0 = 0.6$ - 0.7 , and $SP = 0.5$ gives stable image for several scans. After several scans, the tip can adsorb something from the surface (Eaton, 2010) and it is sometimes necessary to recalibrate the frequency and amplitude.

The amplitude of oscillations in TM AFM is another critical parameter. In our study the oscillation amplitude of 20-800 nm was used in air. The amplitude in liquid was in the range of 10-60 nm. Feedback gain (FB) is an important parameter which shows how quickly piezotube will respond to changes in morphology. It is different in different AFM systems. Usually in Ntegra AFM with P8 controller $FB \sim 0.1$ - 0.5 was used to prevent oscillations and achieve fast enough piezo-response. The scanned area was as large as 135×135 μm for an overall image to check homogeneity. Small 1×1 μm areas were scanned for high resolution images.

3. Examples of different artifacts

In this section, a comprehensive set of experiments illustrating diverse AFM artifacts is provided. The main focus is on organic and biological specimens on diamond substrates. Hard substrates such as diamond can increase the possibility of damaging the tip, yet they provide sound background with tailorable properties for studies of molecules and organic specimens in general (Rezek, Ukraintsev & Kromka, 2011; Hoffmann et al., 2011).

3.1 Artifacts related to the AFM tip and cantilever

The first group of artifacts concerns tip-related artifacts. The AFM sensing element is a cantilever (a flexible plate with force constant k , resonance frequency f and quality factor Q) with a tip (a sharp probe usually with pyramidal shape and radius of curvature r). All these parameters (k , f , Q and r) are important for the measurements.

An AFM image is inherently a convolution of the imaging tip shape with the actual shape of the imaged object (Allen et al., 1992). Thus, whatever is the sharpness of the tip, one will observe broadening of the sample features. For example, the diameter of DNA (2 nm) (Klinov et al., 2009) is much smaller than the tip radius r for ordinary cantilevers (10 nm). Obtained width values are 10-20 nm for dsDNA studied by normal tip (Maeda, Matsumoto & Kawai, 1999), and 2.7-5 nm studied by ultrasharp tips (Klinov et al., 2009).

There is a possibility how to get round this problem, for example one can use ultrasharp tips with tip radii $\sim 1\text{-}2\text{ nm}$. Some of those tips are based on carbon nanotubes (CNT) (Zhao et al., 2008) or diamond-like needles grown under conditions of low temperature plasma in an atmosphere of $\text{CH}_4/\text{H}_2\text{O}/\text{Ar}$ (Klinov et al., 2009). So far, ultrasharp tips cannot be used in liquid because of their relatively high force constant. The development of soft and sharp tips for imaging in liquid would be very helpful for this type of structural analysis (Moreno-Herrero et al., 2004). It was shown that it is possible to make soft AFM cantilevers with a CNT tip, which may be used in liquid, but only measurements in air in CM were shown as an example (I.-C. Chen et al., 2007). There are sharp silicon probes attached to silicon nitride cantilevers which can operate in liquid, but their tip radii r are still about 8 nm (Shekhawat et al., 2009).

Another possibility to reduce the effect of broadening of the picture is to apply the deconvolution procedure to the image (Moreno-Herrero et al., 2004). The deconvolution procedure estimates the tip shape and subtracts it from the topography image. There are two methods how to do it: using a test sample or “blind” mathematical restoration (Keller & Franke, 1993; Dongmo, 1996). Measurements of test samples are useful to estimate real tip shape; however, the resolution of this method is limited to the radius of “tips” on the grating. Moreover, during such procedure, the AFM tip can be damaged. There are several ways how to perform “blind” mathematical restoration. A dilation and an erosion are non-linear mathematical operations consisting in an over- and under-estimation of the tip broadening effect which may help to estimate real object’s shape. There were made several attempts to use other deconvolution methods and find the “real” topography based on AFM image, for example using similar angle identification (Bernardes-Filho & Assis, 2005).

In addition to a simple feature broadening, the AFM tip may have several protrusions, the so called double tip. Double tip is a common effect; it can be divided into double-probe, double-tip, triple-tip effect and so on (Y. Chen et al., 2004). We illustrate this effect on the AHAPS layer on the MCD surface. A periodical structure with the period of $d = 20\text{ nm}$ on AHAPS layer on MCD was observed using a new (out of the box) cantilever (Multi75Al, Budget Sensors) (see Fig. 1a). The first step to check if this is an artifact or not is to change the scan size and scan position. On two consecutive scans, the same periodical structure was observed. But the next scan on a different place without additional changes in scanning parameters didn’t reveal periodical structure (see Fig. 1c). Ultrasharp tips were used on both NTEGRA and Veeco AFM to check that indeed there is no periodical structure. Therefore, we can claim that such periodical structure is an artifact. Hence, even if AFM image is clear and detailed, it still can be an artifact due to tip properties.

For instance, if the tip is damaged during approach or during measurements, one will see repetitive features on the image. The AFM image may contain many triangular features, pairs of features with similar shape and ghost objects (Y. Chen et al., 2004). During approach on AFM in TM, the amplitude of the cantilever oscillations may become zero or much lower than the Set Point value (see Fig. 2). The curves were obtained using NTEGRA AFM, but this effect occurs generally. After approach, the piezotube oscillations can cause oscillations. The optimization of scanning parameters (feedback value, close loop parameters) usually takes some time and during this process oscillations are a common effect. The AFM tip can be damaged during this process.

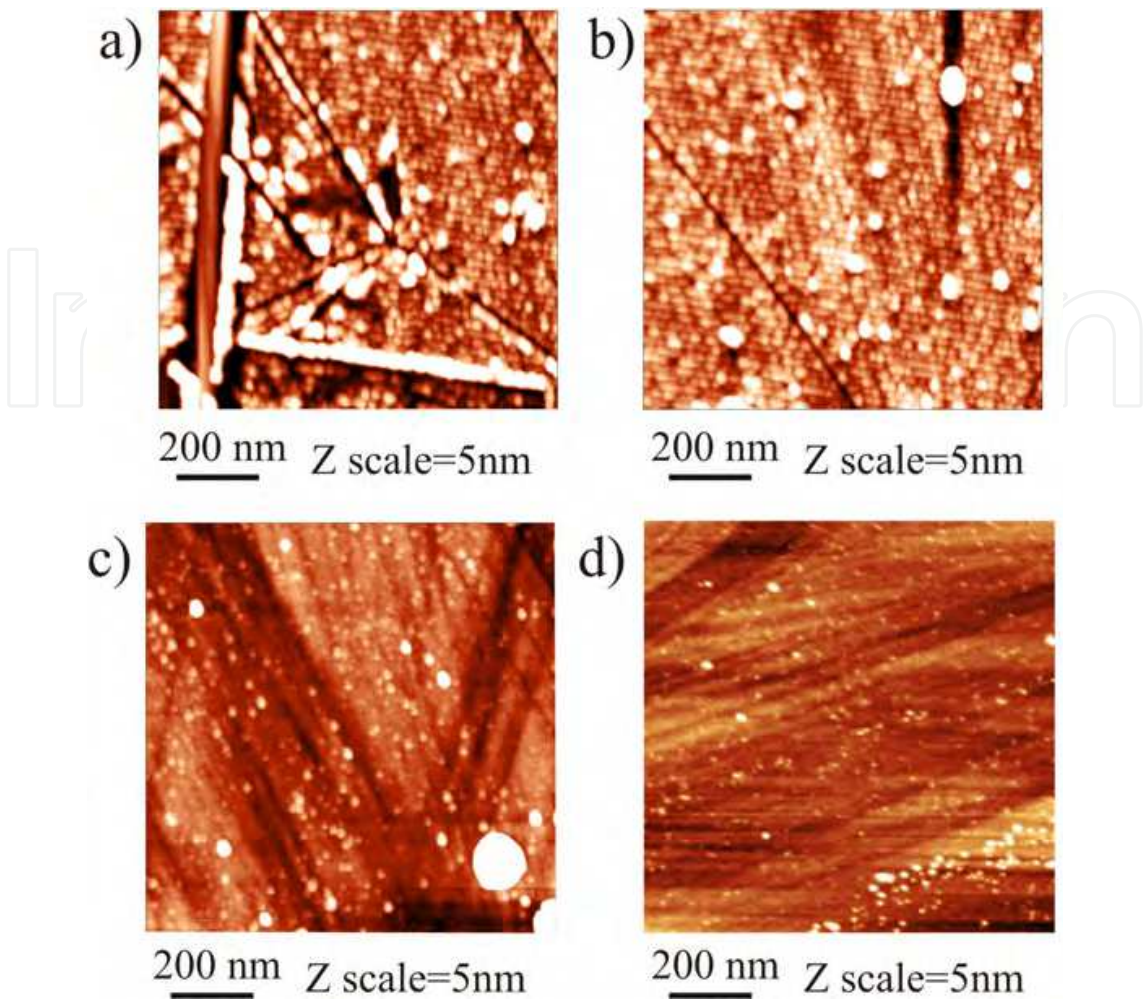


Fig. 1. AFM topography images (1×1 μm) of organosilane layer chemically grafted to O-terminated monocrystalline diamond using Multi75Al cantilever and NTEGRA AFM a) just after approach, b) second scan, c) after several scans; d) The image of AHAPS layer on MCD using ultrasharp tip and Veeco AFM. The images were observed in air.

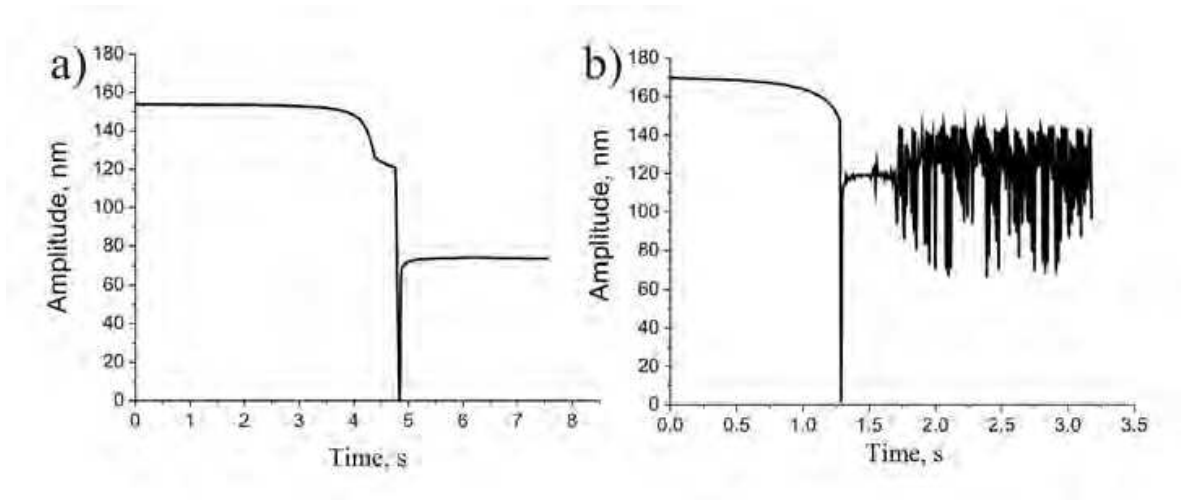


Fig. 2. a) The approach curve on NTEGRA AFM. The amplitude became zero when cantilever touched the surface. b) After the approach, oscillations occur.

During scanning, the tip can be changed due to collisions on the surface. If a scan size is large or the tip does not get blunt after such event, there is no visible change in the topography image, yet big changes in the phase image and even change of the sign can be observed as shown in Fig. 3.

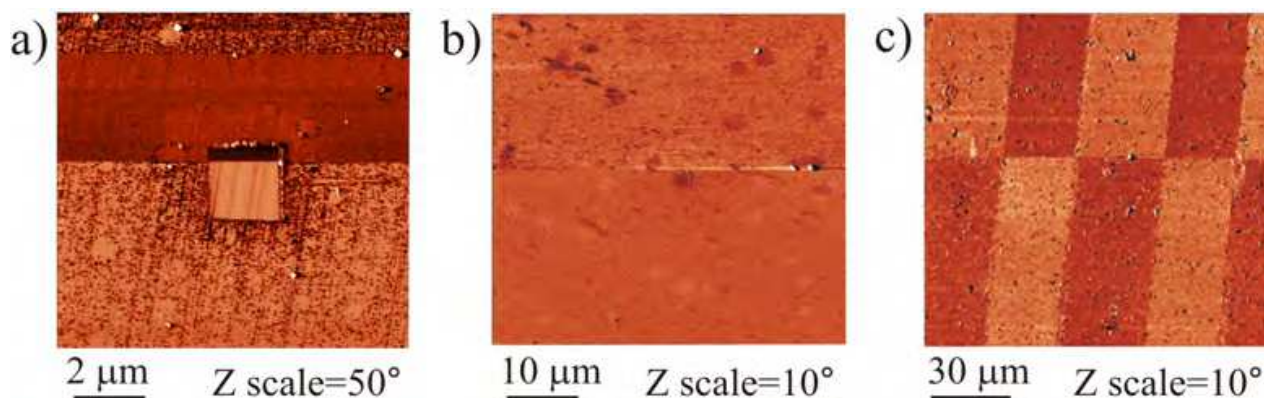


Fig. 3. Phase images were obtained in air and in solution. There is one collision event in each image, which causes some changes in phase image. a) The central 2x2 μm area was nanoshaved in CM. During 10x10 μm overscan in TM, the phase contrast changed to the opposite. b) A large scan (50x50 μm) was made to check the homogeneity of the FBS on MCD sample. At some point, the tip hit something on the surface and the phase contrast changed. c) A 135x135 μm scan was made across 30 μm wide hydrogen and oxygen stripes on MCD with FBS layer on it. At some point, the phase contrast was reversed.

If the object height is large enough (for example bigger than several micrometers) the artifact due to the pyramidal shape of the tip can appear as shadows (Hyde, Jacobs & Compton, 2004). Shadows in AFM images of *Escherichia coli* K12 were oriented in parallel lines 27° from the direction of the cantilever tilt, regardless of the scan direction (Velegol et al., 2003). As another example, Fig. 4 shows the topography of organosilane layer photochemically grafted to O-terminated monocrystalline diamond. This image contains shadows near each cluster and the globular particles do not look like a sphere but rather like faceted crystals.

We have seen that feature width is inherently overestimated in AFM. On the other hand, the height of the soft object is usually underestimated (Rezek, Shin & Nebel, 2007) (0.7 nm for dsDNA (Maeda et al., 1999) or 1.2 nm (Klinov et al., 2009)). This is due to the force which is applied to the sample even during TM scanning which results in elastic deformation of DNA and other polymers.

The force constant of the cantilever k plays an important role in such studies. For stiffer cantilevers, the compression is usually higher than for a soft cantilever. For the lower set point value (SP), the compression is usually higher than for higher SP . In non-contact AFM, lower forces are applied than in TM. This method gives better vertical resolution than TM AFM (Maeda et al., 1999). In this method, AFM tip oscillates near the surface and “the cantilever/tip ensemble is maintained within the long range tail of the attractive surface potential” (Checco et al., 2006). Nowadays, jumping mode AFM (Moreno-Herrero et al., 2004) can be used to diminish the problem of sample deformation and achieve even better resolution, for example DNA height of 1.7 ± 0.3 nm was measured (Moreno-Herrero et al., 2004). This value is close to the real one (2 nm), yet it is still smaller. In jumping mode AFM, force versus distance curves

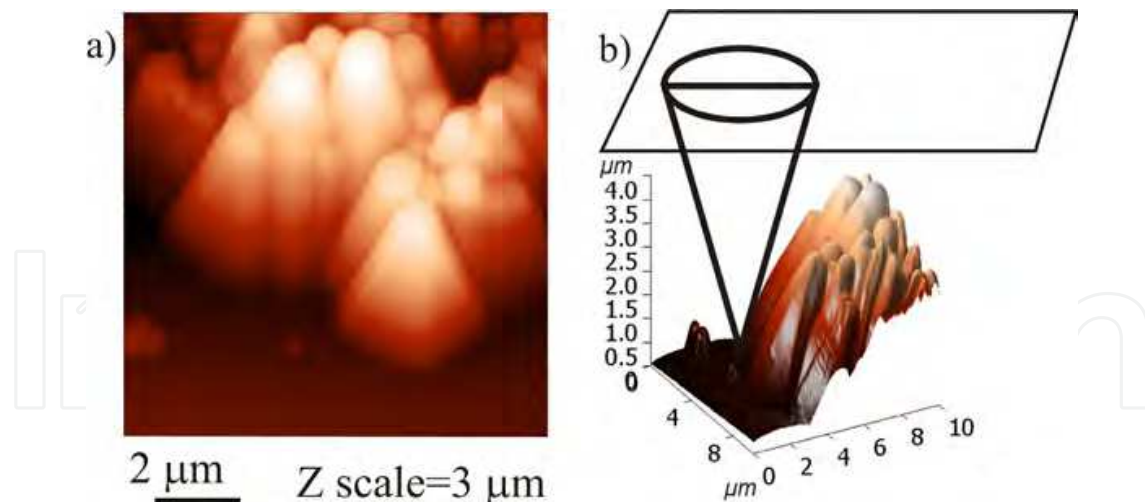


Fig. 4. a) The two-dimensional AFM topography image ($10 \times 10 \mu\text{m}$) of the organosilane layer photochemically grafted to O-terminated monocrystalline diamond. b) The same data presented in a 3D image with a model of AFM cantilever with finite cone angle. Images were made using Multi75Al cantilever and NTEGRA AFM.

are measured at each point of the measured surface with applied feedback in between. The non-contact and jumping mode AFM are technically challenging methods compared to tapping or contact mode and they are not generally applicable.

Also the resonance frequency of a cantilever plays an important role. Steps in height up to 200 nm were observed at a boundary of H- and O-terminated surface region on MCD in solution using soft cantilever CSG01 oscillated in TM (Rezek, Ukraintsev & Kromka, 2011). This is artificial as the real height difference between H/O surfaces is smaller than 1 nm, as obtained using medium frequency NSG01 and Multi75Al cantilevers both in CM and TM. For soft cantilevers such as CSG01 (which properly work in air at $f \sim 30 \text{ kHz}$), measurements in TM in solution are not recommended, because oscillations at the first resonance frequency become small and measurements at the second harmonic may cause incorrect height determination (Rezek, Ukraintsev & Kromka, 2011). Nevertheless, higher harmonic oscillations can be used to study stiffness of the material (Sahin et al., 2004).

New AFM methods may appear in the nearest future, for example based on very soft polymers cantilevers (Calleja et al., 2005). True atomic resolution imaging of muscovite mica by a frequency modulated atomic force microscopy (FM-AFM) in water was recently demonstrated using a low noise all-fiber interferometer as the deflection sensor (Rasool et al., 2010). Contact resonance imaging (force modulation mode) is applicable for measurements of soft and sticky samples because in this case the sample and the tip are always in contact (Wadu-Mesthrige et al., 2001). Combined frequency and force modulated AFM was suggested but not tried yet (Solares, 2007). Amplitude-modulated AFM was used to determine the morphology and the compositional variations of surfaces in their natural environment. The applications in biology, polymer science and microelectronics illustrate the potential of phase-imaging force microscopy for nanoscale analysis (Rezek, Shin & Nebel, 2007; Garfias-García et al., 2008). Magnetic alternating current mode AFM is a very useful tool to image soft materials in liquid, where ordinary TM is difficult due to poor resonance of the cantilever (Ge et al., 2007).

The AFM cantilever can cause artifacts not only due to the tip shape and force constant, but also due to the lever shape and the laser light position. For example, experimental results show a nonlinear relationship between the detected signal and the actual deflection of the cantilever. There are at least 8 possible sources for such nonlinearity, but the main reason of this artifact is the shape and intensity distribution of the laser light hitting the detector (Thormann, Pettersson & Claesson, 2009). If the sample is too bright and the laser spot is too large, one can see laser interference patterns. Readjusting the laser or using low-coherence laser sources can reduce this problem (Eaton, 2010).

3.2 Artifacts related to the AFM scanner

Another group of artifacts are those related to a piezoscanner that moves the tip and/or sample in AFM. The piezoelectric creep and edge overshoot are well known artifacts (Eaton, 2010). For example, just after setting up the tip, adjusting laser, setting sample and approaching the tip to the sample one can observe piezoelectric creep and changes in the oscillation amplitude of the tip. The best way to solve these problems is to wait for some time (up to 30 min). After reaching equilibrium, these problems will disappear in most cases. These problems are smaller, yet still present with an active closed loop scanner system. The active closed loop can also cause additional piezotube oscillations, which sometimes makes it impossible to use high feedback values needed for efficiently fast tracking of the surface and therefore should be switched off in such cases.

In the case of a commonly employed piezotube scanner, the piezoelectric tube bends during measurements and this effect causes z position error and introduces background curvatures. For flat samples, it is easy to correctly subtract the artificial curvatures, but for patterned structures with big feature height it is very difficult. The degree of curvature depends not only on the scan size and scan speed, but also on the x - y offset and z position, making it impossible to correctly subtract the curvatures.

When scanning feedback gains are too high, the scanner can oscillate, generating high-frequency periodic noise in the image, which is sometimes even audible. This may occur throughout the image or be localized to features with steep slopes. However, when feedback gains are too low, the tip cannot track the surface, and features will be distorted and smeared out (Ricci & Braga, 2003). With a low feedback value and quite fast scanning speed, the piezotube response in z -direction is not fast enough, so one can observe different object shapes depending on the scanning directions.

An example of this problem is presented in Fig. 5, where oscillations at $FB = 0.1$ are clearly visible and they do not disappear after lowering the feedback to $FB = 0.05$. At this value, the feedback does not follow the surface well. So, no good image can be obtained in such conditions.

Other effects from this group are thermal drift and hysteresis nonlinearity. AFM with three dimensional feedback control loops are able to minimize these effects, but these feedback controllers are often not designed to deal with the highly resonant nature of an AFM's scanner nor with the cross coupling between various axes (Mahmood & Moheimani, 2009). The extension of features in the scanning direction, positive and negative noise peaks, positive and negative sticking effects were presented (Gainutdinov & Arutyunov, 2001).

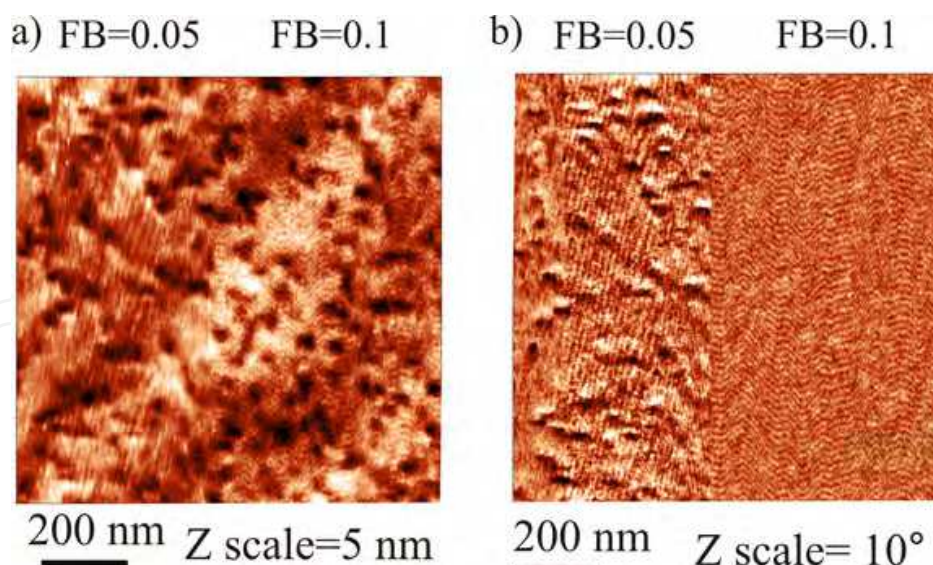


Fig. 5. The AFM image of FBS layer on MCD surface was measured in solution using Multi75Al cantilever and NTEGRA AFM. At $FB = 0.1$ oscillations, which reduce the quality of the image, were clearly visible. At $FB = 0.05$, the oscillations were still visible, and features were distorted. a) topography image, b) phase image.

3.3 Artifacts related to the sample properties

The next group of artifacts appears due to specific properties of a sample. For example, the sample can drift in one direction even if it is well attached to the sample holder. If this drift is due to thermal drift, one can reduce it by stabilizing the temperature. If it is due to other reasons, one can scan faster (Eaton, 2010). If the sample is too sticky or too soft, an artifact due to multiple probe-sample contact points occurs (Morton et al., 2003; Sokolov, 2007). This problem is highly relevant to cells studies (Touhami, Jericho & Beveridge, 2004). If the sample is nonconductive, electrostatic charge can be stored and generate long range forces, and the AFM image may thus not correspond to topography (Miyazaki et al., 2000; Verveniotes et al., 2011). Note that the charge distribution measured by Kelvin force microscopy may not fully correspond to real charge distribution (Lambert et al., 2003).

3.4 Artifacts related to the interaction between tip and sample

The last group of artifacts is related to the interaction between the tip and the sample. One such well known effect is a “contrast reversal” artifact. The artifact occurs when the oscillating cantilever is in an attractive or repulsive mode according to the dominant tip-sample interaction mechanism (Kühle et al., 1998). If during scanning the attractive regime switches to the repulsive one, one can observe strange contours, unexpected height shifts, and changes of the apparent resolution in the acquired images. Contact resonance imaging (Wadu-Mesthrige et al., 2001) may be a good replacement of TM in that case.

Fig. 6 shows an example of the “contrast reversal” artifact during measurements of the AHAPS layer on the MCD surface using an ultrasharp AFM tip and very soft tapping mode ($SP = 0.98 \cdot SP_0$). It looks like there are holes in the center of high objects. The explanation is that in some points AFM changes regimes from a repulsive to an attractive one and then

back again to the repulsive. SP/SP_0 may differ across the sample, thus this artifact may be present only in one part of the image.

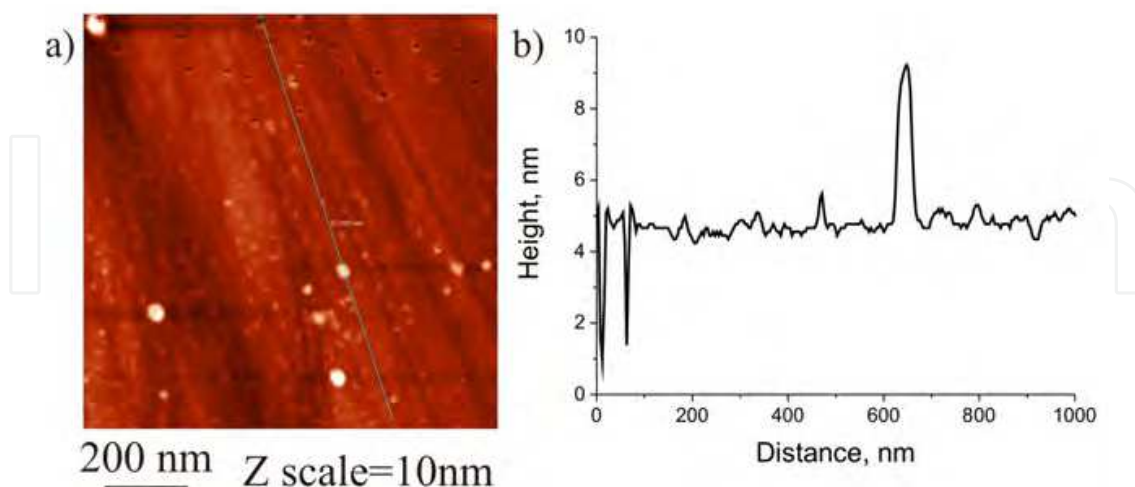


Fig. 6. The AFM image of the AHAPS layer on the MCD surface was observed using ultrasharp tip (NTI Europe). At the top part, a lot of 5 nm objects look like 2-3 nm holes on the surface. This artifact is due changes from repulsive to attractive regime. Usually conditions for such effect are $SP_0 \sim SP$, $SP > SP_0$ at the top part and $SP < SP_0$ at the bottom part.

Another example was observed on the FBS layer on the MCD sample as shown in Fig. 7. At the bottom part of the image, SP is setup a bit lower than SP_0 and the measurements are carried out well. But during scanning the tip accumulates something on it and gets heavier. This causes a drop in A_0 and, therefore, increase in SP . Fig. 7 illustrates the frequency shift and amplitude reduction during measurements. ΔA indicates a drop in the amplitude of oscillations due to the adsorption of material on the tip. Eventually, SP will be equal to SP_0 and the image will be blurred or even the intermittent contact will be lost. This means that one should change SP value correspondingly to changes in SP_0 . Such artifacts may appear during AFM study especially when measurements are performed in liquid, where the Q factor of cantilever is low, and on a soft material, which can be easily removed by tip.

The contamination of the tip should be considered in nanoshaving experiments that are used to study thin protein layers (Rezek et al., 2009). In this method, the first image is made in CM, and second is made in TM. One can obtain deep hole in the layer, but if one continues to perform TM measurements, one will observe the reduction of the layer height due to the tapping mode nanoshaving (Rezek, Ukraintsev & Kromka, 2011). If the bottom surface is not very clean or well visible, one can think that the hole is filled with proteins. Only larger overview scan can prove that there is no such effect. The easiest way to define the layer height and get around this problem with tapping mode nanoshaving is to use a single TM scan with small amplitude.

The tapping mode nanoshaving effect can also cause blurring of the topography images. In this case, the layer is partially destroyed during the first TM scan. Tapping mode nanoshaving leads to blurring of the image.

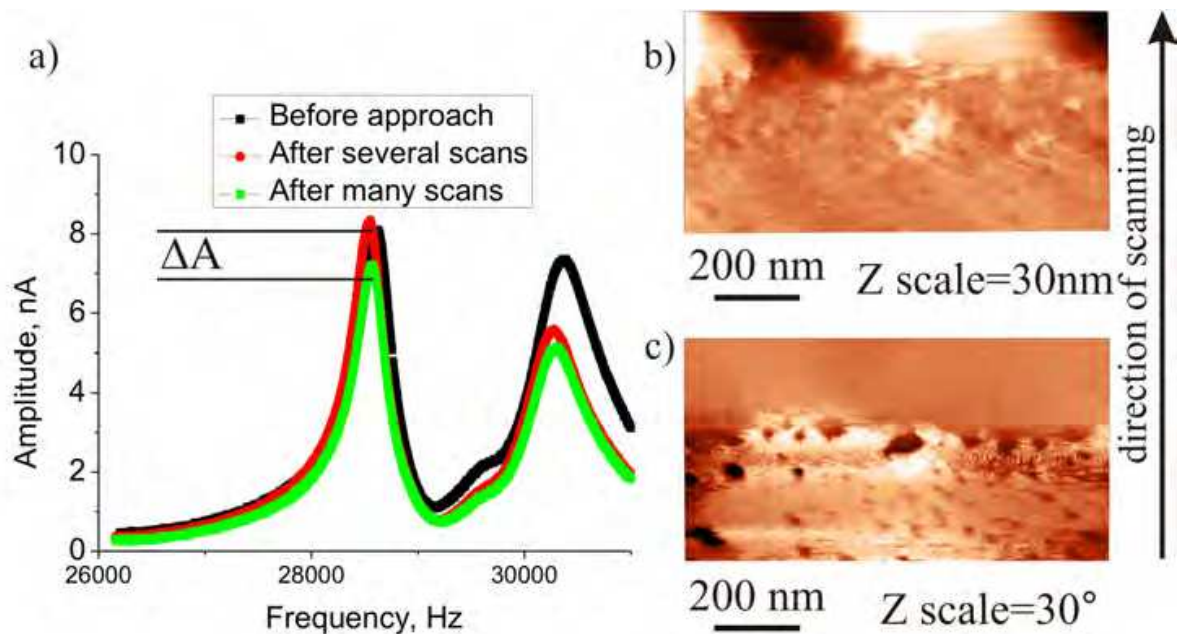


Fig. 7. The AFM morphology of the FBS layer on the MCD surface measured in solution. a) The frequency shift for Multi75Al cantilever for imaging in solution. b) The tip loses contact due to decrease of the oscillation amplitude. The topography image became blurred. c) The phase image illustrates loss of the phase contrast after SP reached SP_0 .

It is important to make a high resolution scan before making an overall image, because the tip may become blunt during the overall scan. The proper order is to make two high resolution images on two differently terminated areas of the surface, for example H- and O-terminated diamond surfaces, and then to define the position of those areas using the big scan. The problem which usually occurs is that it is not possible to find out where the initial fine scans were made, because positions of fine scans were too close to the H/O-border.

A very important factor for AFM imaging is also the tip surface chemistry. If the tip is not contaminated, but its surface has been modified, for example with liquid 1-decanethiol, this tip will not work the same way as a clean tip (Nie & McIntyre, 2007). It was observed that in this case the cantilever amplitude will be unstable and AFM images become noisy. Under such conditions, the amplitude change is dominated by the extra forces induced by the active material loaded on the tip apex, overwhelming the amplitude change caused by the geometry of the sample surface, thus resulting in noise in the image (Nie & McIntyre, 2007).

In the case of tip contaminations, the debris particles may partially detach from the tip and may, during the scan, leave a diagonal track in the image that could be erroneously interpreted as a surface feature. Telltale signs in this case are the instabilities and glitches in the feedback signal that occur each time the particle is dragged along (Ricci & Braga, 2003). Fig. 8 is an example of such an effect. In this case, dust particles were moved on the MCD surface during a measurement. Traces of the dragged particles are clearly visible in the phase image (Fig. 8b), in contrast to the topography image (Fig. 8a).

During scanning one should keep SP a bit lower than SP_0 to obtain good contact and to avoid high pressure. However, SP_0 is often much lower than the recommended SP value for

scanning, e.g. with ultrasharp tips (NTI Europe) and NTEGRA AFM (NT-MDT) $SP_0 = 0.7$, while recommended $SP=0.95$. This means that one may break the ultrasharp tip even before getting the image. Blurred images may be obtained with high SP ratio (recommended value) and increased interaction between the tip and the surface will break the very tip.

One of the most important artifacts related to the tip-sample interaction is the flying tip artifact (Eaton, 2010). In this case feedback loop is not adequate and the tip does not follow the sample. Usually increase in feedback gain, reduction of the setpoint and slowing down the scanning speed helps. But if not, which is often the case when studying soft protein layers, there is no straightforward solution to this problem. For example, it is difficult to obtain good images of weakly attached cells due to the interaction between the cantilever and the cell membrane. Another possible reason for bad contact between the tip and the sample is the electrostatic interaction between the tip and the sample, as in the case of charged sample which was described in Section 3.3. The grounding of both conductive and not conductive samples usually helps in this situation.

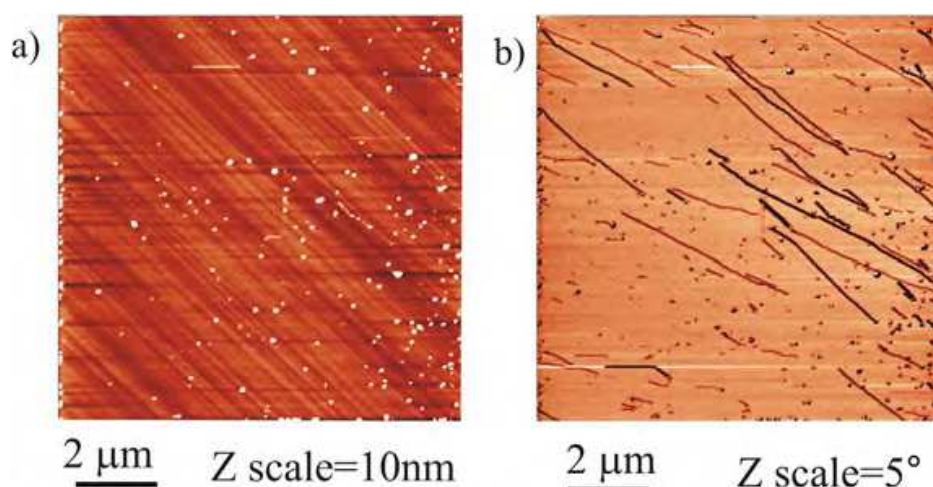


Fig. 8. AFM micrographs of the MCD surface which was dirty after insufficient cleaning. The dust was easily moveable on the surface when using TM AFM. The linear traces are observed in the phase image (b), but not in the topography (a).

3.5 Artifact related to the interference between specimen grating and the scan raster of AFM

AFM artifacts can usually be easily discerned in the images. But sometimes, well looking AFM images may be an artifact as described in Section 3.1. For example, there are a lot of publications where images with moiré – interference between the specimen grating and the scan raster of the AFM (Su et al., 2005) – are shown and ways to remove them are proposed. In this case, the topography image does not correspond to the real topography of the specimen.

An example of the moiré artifact on MCD surface measured in TM is presented in Fig. 9. This wave structure is not reproducible and direction of waves depends on scanning parameters. Therefore we can claim that this wave structure is the moiré artifact, not topography.

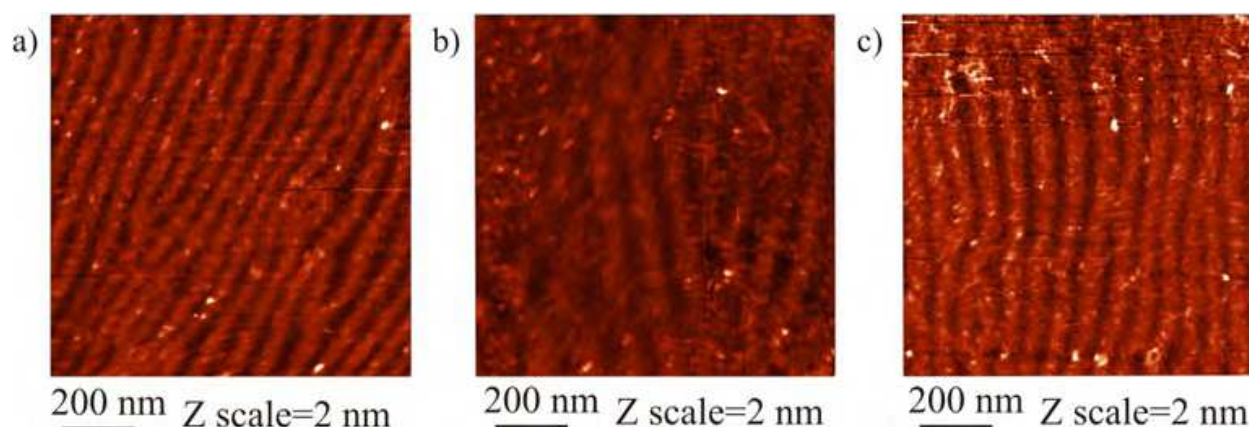


Fig. 9. The MCD surface was measured in TM with different parameters: a) horizontal scan, $SP = 0.69$, b) vertical scan, $SP = 0.69$, c) horizontal scan, $SP = 0.65$.

4. Solutions how to avoid artifacts

4.1 The tip shape

The first step which one has to do to obtain an AFM image is to approach the surface. This initial tip approach to the surface must be performed carefully as the approach itself may “crash” the tip even in TM (see Fig. 10). One should monitor the amplitude during the approach so that it does not drop to 0. Fig. 2a shows that the amplitude of oscillations drops to 0 and the tip runs into surface. If the feedback value is too high during approach, the tip will start to oscillate immediately after the tip-surface interaction is established (“contact”) (see Fig. 2b). These oscillations may damage the tip as well. After these events, the tip may become blunt. To estimate the force which is applied to the tip during this event one can assume that the tip is pressed against the surface for a distance equal to the expected amplitude. Roughly, this corresponds to the force which is applied to the cantilever during CM measurements, for example ~ 600 nN for NSG cantilevers.

The best way to get around this problem is to do approach in several steps. First, a fast approach with $SP > SP_0$ for ordinary cantilevers should be made. At this point, the cantilever starts to feel the surface and its resonance frequency changes. After that, it is important to make tuning of the cantilever again to adjust the amplitude and the frequency and make the approach again with the required set point and lower speed. “Safe” approach on the final step is also recommended. Contact mode approach is not recommended because of the high force applied to the tip during the first contact with the surface.

Tapping and contact mode approaches can be less destructive for the tip if used in the “safe” approach mode, where, after each step made by the motor, the piezotube extends and shrinks back and the software checks whether the set point is already reached and only after that if it is safe for the tip the next step by motor is made. Although safe for the cantilever, it is a slow way to approach the surface.

Just after approach, the tip quality is usually the best and therefore the image quality is the best one can achieve with that particular tip. This means that the first images are the most important. For example the result presented in Fig. 1 shows a periodical structure which was observed during the first and the second scan. That periodical structure maybe a real

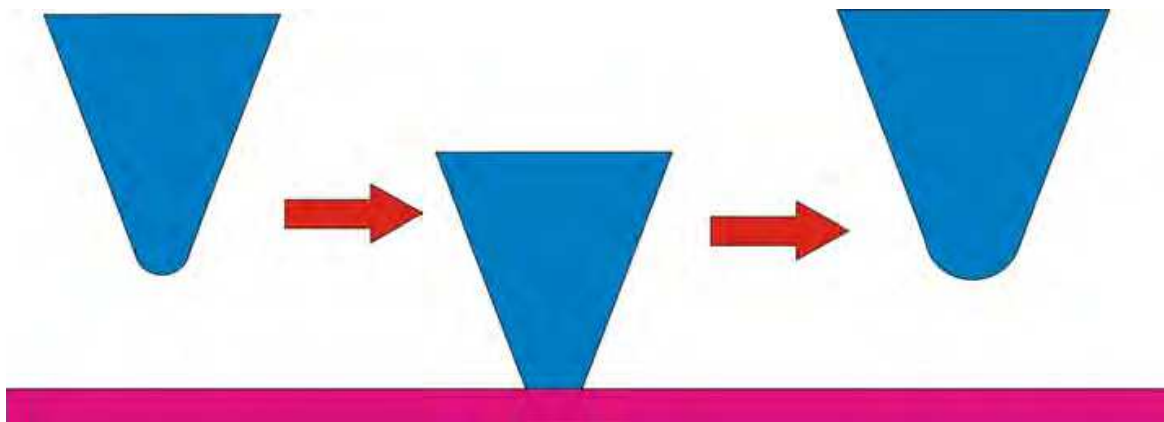


Fig. 10. A cantilever runs into surface during approach. After such event, it may get blunt.

structure and the tip has a needle which was extremely sharp (Fig. 11a), but since neither an ultrasharp tip (NTI Europe) using both NTEGRA AFM (Fig. 1c) and Veeco (Fig. 1d) later could see such periodicity, nor SEM resolved it, we have concluded that this structure is an artifact. Moreover, features are not duplicated and this periodical structure disappears after several images yet the quality of the image was quite good, i.e. the tip did not become blunt. Therefore, this should be an artifact of the tip. The main reason for such an effect may be a doubled tip, but this case is more complicated, because there is a fine scratch (black line) which is not doubled and there are also a lot of AHAPS clusters which are single. Fig. 11 illustrates two models which may explain such a periodical structure with single line. There is small probability that the Multi75Al tip was very sharp ($r \sim 1$ nm) after approach and there is such fine structure on the surface. After several scans tip radius increased up to $r \sim 10$ nm and periodical structure became invisible. But most probable version is that the tip had two or four sharp needles and after several scans one of them broke.

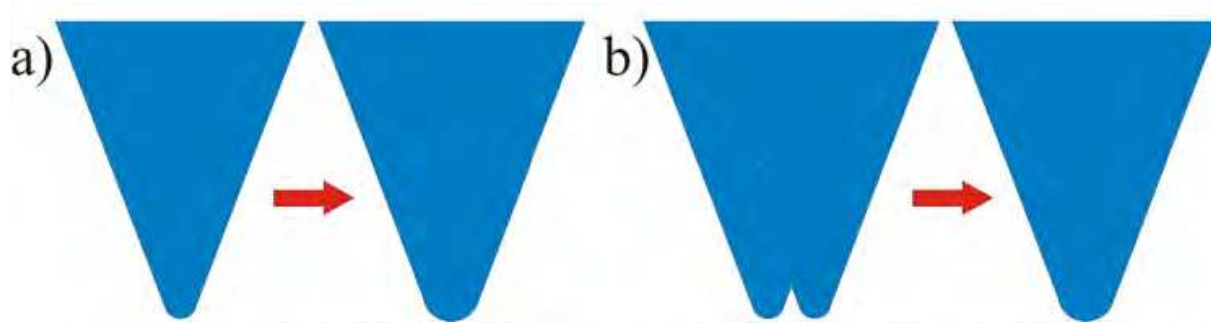


Fig. 11. Two models which may explain periodical structure. a) The extremely sharp tip Multi75Al (nominal $r = 10$ nm) which is sharper than ultrasharp tip (NTI Europe) became normal tip ($r = 10$ nm) after collision. b) Double tip with sharp needles became normal tip after collision.

The changes in tip's shape during measurements are very important to watch for. In Fig. 3 several phase images with collision event are shown. Such events usually occur when the tip hits a high object on the surface. When the tip hits such an object, it can become blunt or it can dislodge particles from the surface and these particles can become attached to the tip (see Fig. 12). In this case, the mass of the tip is changed, leading to changes in the resonance frequency and the amplitude of oscillation and, therefore, to offset in phase shift between

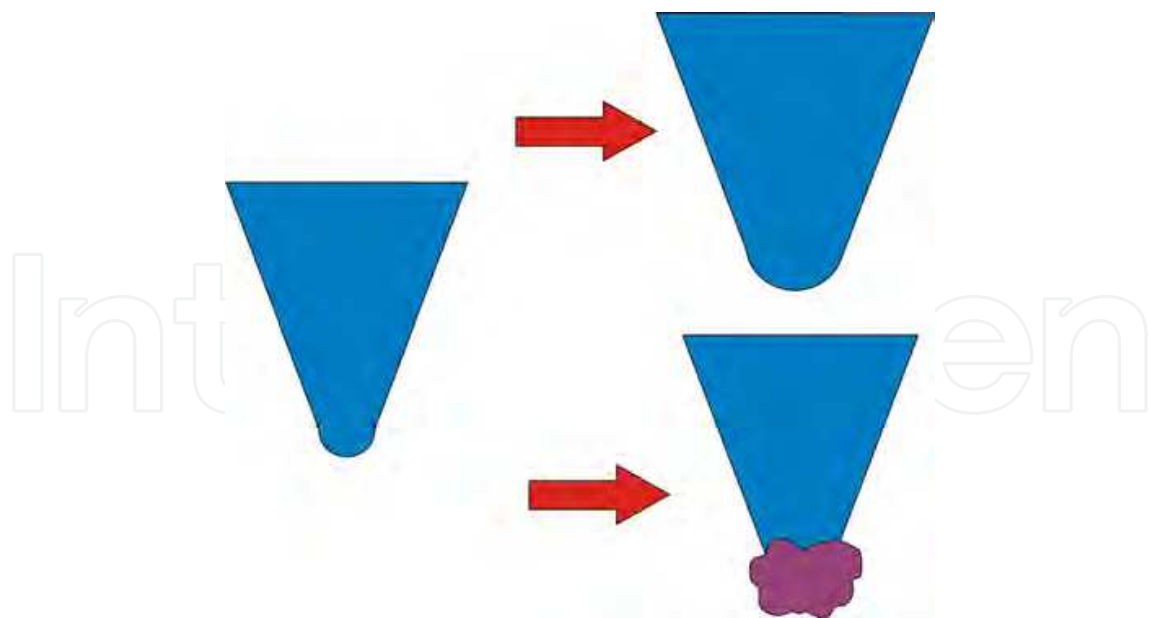


Fig. 12. Collision events, which can cause some changes in phase image. The tip can become blunt or it can dislodge particles from the surface and these particles can become attached to the tip.

the resonance and the driving frequency. The changes in surface chemistry (e.g. protein on the tip surface) can cause different energy dissipation and, therefore, changes in the interaction between the tip and the surface and also changes in the phase contrast. On the other hand, if the tip does not become too blunt or the scan size is quite large, no changes in the topography will be observed. There is no general way how to avoid such effects, except for avoiding sharp and/or hard features on the surface.

As the changes in the tip shape can cause reversal of phase contrast, it is important to somehow calibrate the phase contrast during the measurements. One possibility is to have standard objects on the surface with a known phase contrast and measure them before and after the experiment. Another possibility is to use the same tip for all the measurements and monitor whether the tip has changed or not. Since after several images the tip may get blunt, it is better to use diamond or diamond-coated tips to control the phase contrast.

If the tip radius is bigger than the object size, the tip broadening effect will occur and the object will appear bigger than it is (Rezek, Ukraintsev & Kromka, 2011). If the tip radius is bigger than the distance between the nearest objects, the tip does not touch the substrate between the two objects and, therefore, both objects will be recognized as one bigger object (see Fig. 13b). The best way to avoid this artifact is to use sharp tips with r lower than the average feature size.

There are two main parameters which define the tip shape: the tip radius and the pyramidal or cone shape of the tip. The latter can cause an artifact when the tip is used to study high features. In Fig. 4, one can see that different objects have similar edge shape. The main reason for this effect is the tip shape, i.e. that the cone angle is not zero (see Fig. 14). The best way to avoid this artifact is to use cantilever with aspect ratio as high as possible.

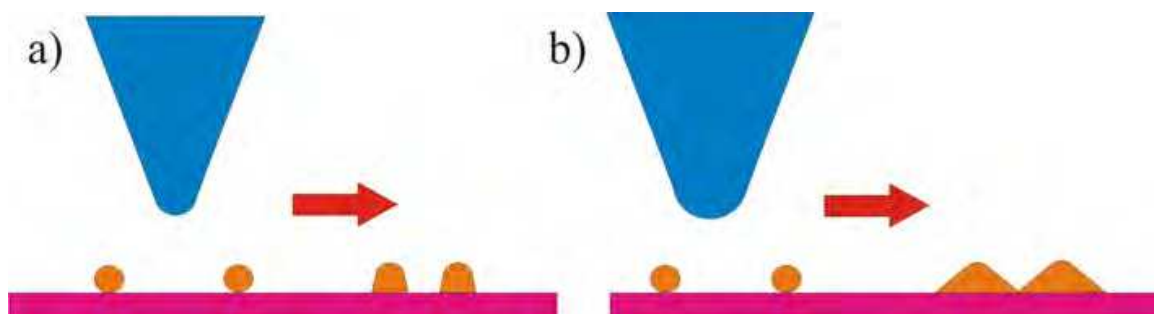


Fig. 13. The tip broadening artifact. a) In case of a sharp tip, the object looks slightly bigger than it is. b) In case of a blunt tip, objects look much bigger than they are, two objects may look like one large object.

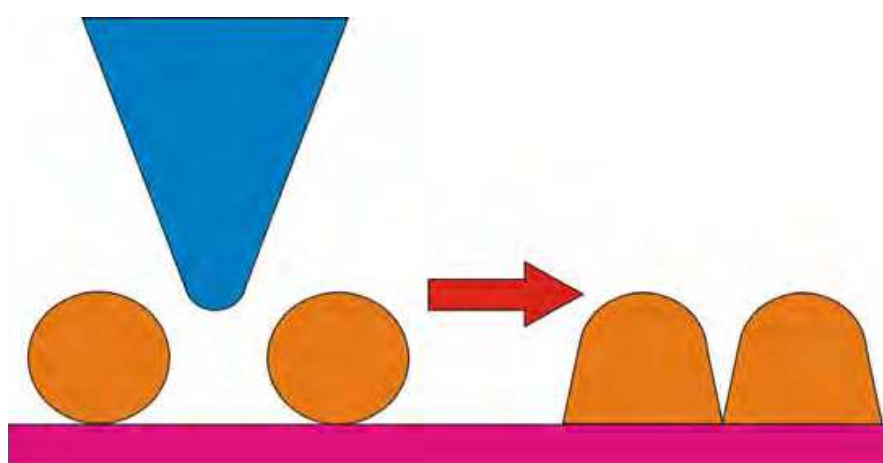


Fig. 14. The model which described edge shape of high object based on tip shape and finite cone angle.

It was shown that the tip is the main part of AFM which determines the image quality. The sharpest tips are seemingly the best choice, but they have a lot of disadvantages in particular for studies in biology. For example, most of the ultrasharp tips cannot work in solution. NP-STT cantilevers from Veeco have a second, shorter tip which is also formed near the main tip as result of the process used to create the sharper tip. Those cantilevers should be used for flat samples otherwise one will observe “twins” due to the double tip. For ultrasharp cantilevers used in air in tapping mode, $SP \sim 0.95$ should be used, so the strength of the tip does not allow any measurements in CM and nanoshaving. If the radius of the tip is small, it can penetrate the cell membrane (H. You, 2000). Ultrasharp cantilevers are also significantly more expensive than ordinary cantilevers.

There are several methods that can improve the tip quality. When the tip is hit against the surface it becomes better (sharper, without double tip, etc.) or it will become blunt. The easiest way to hit the surface is to cause strong tip oscillation close to the surface for example by increasing feedback gain ($FB = 2-10$). To improve the quality of a contaminated tip one can use UV-light treatment that produces ozone and removes organic debris (Thundat et al., 1993), piranha solution (mixture of sulfuric acid and hydrogen peroxide) (Lo et al., 1999), hydrogen, oxygen and argon plasma etching (Chapman, 1980) or CO_2 snow which removes organic debris from the surface because of a transient formation of liquid CO_2 (Hills, 1995).

4.2 The cantilever spring constant k

The choice of a cantilever spring constant depends on a particular system under study. For various applications cantilevers with different spring constants should be used. One can use very soft cantilevers ($k \ll 0.01$ N/m), sometimes made from polymers, for biosensor applications (Calleja et al., 2005). Usually those cantilevers do not have any tip. The working part of the cantilever is its whole surface, which can be modified and used as a sensor for example to study the interaction between lysozyme molecules (Ukrainsev et al., 2007).

Soft cantilevers ($k = 0.06$ N/m) are typically used for force spectroscopy measurements (Kransnoslobodtsev et al., 2005). When these cantilevers are used to study topography several artifacts can appear. Due to low resonance frequency, these cantilevers have low quality factor Q , especially in solution, so these cantilevers do not oscillate well on the first resonance frequency and one has to use the second harmonic, which causes an improper height determination (Rezek, Ukrainsev & Kromka, 2011). For samples with properties similar in every point it usually does not cause any problem and even higher resolution can be achieved than when measuring on higher harmonic (Giessibl, 2006), but for samples with different surface chemistry it may not work. To avoid such artifacts, stiffer cantilevers should be used.

The cantilevers with spring constant $k \sim 1$ N/m can be used to study living cells in-situ (P. Chen et al., 2009). Such tips are often the best choice for nanoshaving experiments on biological samples.

The stiff cantilevers with high spring constant ($k = 40$ N/m) are usually used in air for most of the studies. Sometimes they are too stiff and easily penetrate protein layer or cell (Kwon et al., 2009).

The even stiffer cantilevers ($k = 120$ N/m), for example made from diamond, can be used on hard samples or for cutting of biological material (H. X. You & Yu, 1999). Such tips are often the best choice for nanoshaving experiments on chemically synthesized samples with high layer rigidity, on which the interaction between the layer and the substrate is much higher than for biological samples.

The pressure applied to the sample depends on the applied force and the active surface area, i.e. the tip shape. One needs to take care of the tip shape, because blunt tips will change the forces and pressures needed for cell penetration.

The stiffer the cantilever, the more energy injects the tip to the sample during each approach cycle. This energy is equal to $\Delta E = 2\pi^2 c_t A^2 f$, where c_t is the total damping coefficient, A – the amplitude, and f – the frequency (S.-M. Lin & C.-C. Lin, 2009). The total energy of the tip is $E = \frac{1}{2}kA^2$. Q factor is defined as $Q = 2\pi E/\Delta E$ and drastically depends on a medium due to changes in c_t and depends on the distance between the tip and the surface (Naik, 2003). In liquid, usually $Q < 10$, but if only part of the tip is inside the liquid, Q may reach 100 (LeDue et al., 2009). The decrease in frequency and Q factor is typical for cantilevers in liquid compared to vacuum or air (Reed et al., 2009).

For example, cantilever with $k \sim 3$ N/m and $A \sim 60$ nm has energy $E \sim 10^{-15}$ J and therefore injects $\Delta E \sim 10^{-16}$ - 10^{-15} J per cycle. If energy E is high enough (for example $E \sim 10^{-15}$ J for an

FBS layer or weakly attached cells) to move objects on the surface, this cantilever will remove the protein layer or move the weakly attached cell. In air, Q is higher and ΔE is lower than in liquid. This means that stiff and very stiff cantilevers ($k \sim 40$ N/m) may be used in air, but not in liquid for soft matter on hard surfaces.

4.3 The amplitude of cantilever oscillation A

If the amplitude of cantilever oscillation A is increased the quality factor of cantilever oscillation Q is also increased. This is very important when study is performed in liquid ($Q < 10$). With low amplitude ($A \sim 10$ nm), it is difficult to get stable performance of AFM and make a good image. The increase in amplitude will lead to better resolution and lower noise, but will also increase the size of the smallest object which can be observed. This is the reason why all studies on subnanometer scale are performed with very low amplitude and often in UHV. In some cases, the RMS signal instead of the MAG signal for feedback signal in TM allows one to obtain a better image.

Measurements with high amplitude may result in tapping mode nanoshaving (Ukraitsev et al., 2009). To avoid this artifact, softer cantilevers or smaller amplitude should be used. But softer cantilevers may cause the “contrast reversal” artifact, and smaller amplitude may reduce the resolution of the image. Hence, a compromise must be found in each specific case. For protein-diamond samples studied in solution, cantilevers with $k \sim 3$ N/m and the amplitude of oscillation 10-60 nm are the optimal choice.

4.4 The set point value SP and the feedback value FB

Small changes in the AFM set point can dramatically change the acquired image due to changes between the attractive and repulsive modes, i.e. the “contrast reversal” artifact. To avoid this artifact, one should use a lower SP value. On the other hand, a switching vibrating cantilever mode was proposed to enhance the contrast on flat multi-phase samples as switching depends on the difference in the material properties of the phases (Kühle et al., 1998). A switching vibrating cantilever mode is similar to jumping mode AFM (Sotres et al., 2007). It is based on placing the feedback set point in the repulsive electrical double-layer curve just before the mechanical instability occurs, i.e. there is no mechanical contact between the tip and the sample at any time. This method was used to image single biomolecules in aqueous media (Sotres et al., 2007).

It is often recommended to use a set-point value as high as possible (close to SP_0), but this is relevant only for the measurement on “clean” samples, from which nothing can become attached to the tip. When measuring in solution on soft matter, the best way to avoid this effect is to use $SP \sim 0.9 * SP_0$ and slightly reduce SP if image gets blurred. It is not recommended to use very low SP value because in this case the imaging is invasive and image gets blurred due to the interaction with tip.

It is also important to choose the appropriate scanning feedback value. This is not straightforward, because the reduction of the FB value may cause blurring of the topography image, but increasing may lead to oscillations and additional noise on the topography image and even to loss of the contrast in phase image.

4.5 Measurements of tall features

The scanning range, the image mode and the tip shape influence such cell characteristics as cellular volume and ultrastructural roughness (Wu et al., 2008). True morphology can be partially reconstructed using procedures based on tip shape estimation (Keller & Franke, 1993). In many cases the simple mathematical procedure such as subtraction of the smoothed data from the original data greatly improves the image contrast and quality (Kienberger et al., 2006). This method is applicable not only for tall objects, but also for small particles on a flat surface.

For measurements of tall features with height close to the range of the Z-scanner piezotube, one can use the following technique. Usually AFM is adjusted to the middle of the Z-scanner range after the tip is approached to the surface. For flat and leveled samples this means that only half of the range of the piezotube is available for height measurements. For tall objects, it is thus better to level the sample first and then to approach so that the whole range of piezotube can be used to measurements.

5. Conclusions

Various AFM methods and literature data relevant to the characterization of biological specimens were reviewed in this chapter. Diverse AFM artifacts that arise during AFM characterization of such soft matter samples were illustrated by measurements of FBS proteins and AHAPS linker molecules on diamond substrates. The artifacts were divided into four categories: artifacts related to the tip, to the scanner, to the sample and artifacts related to the interaction between them. Various effects in AFM morphology and AFM phase data were demonstrated and their physical origins were explained based on the schematic models.

Possible artifacts related to feature height and other specific structural, chemical, and electronic properties of the samples were considered. Sub-nanometer roughness of monocrystalline diamond substrates provided well-defined background for the AFM study of organic molecules. Moreover, the possibility of tailoring diamond surface properties by modifying surface atoms and linking molecules (for example AHAPS with NH_2 groups) opens prospects for broader applications in biological studies.

The influence of the tip shape, cantilever spring constant, amplitude of tip oscillations, feedback and set point values on the reliability of AFM characterization were also discussed. We showed how to choose a proper cantilever depending on the specific sample and characteristics of interest. Every cantilever has its own application area. In summary, soft cantilevers ($k \sim 0.06 \text{ N/m}$) are the best choice for force spectroscopy measurements and stiffer cantilevers ($1\text{--}120 \text{ N/m}$) should be used for nanoshaving experiments on biological and chemically synthesized samples. Cantilevers with $k \sim 3 \text{ N/m}$ are the most suitable for *in-situ* measurements of proteins (Rezek, Ukraintsev & Kromka, 2011). Several further guidelines how to obtain reliable AFM characteristics of molecules and cells were presented. Different ways to avoid artifacts such as tapping mode nanoshaving, negative contrast, or image blurring were described. The presented work may thus help researchers to optimize and better understand AFM measurements and to avoid incorrect conclusions.

6. Acknowledgements

We would like to acknowledge a kind assistance of V. Jurka with photolithography, Z. Poláčková with chemical treatment, O. Babchenko and J. Potměšil with hydrogen plasma treatment, and M. Kalbacova for protein donation. This research was financially supported by AV0Z10100521, research projects KAN400100701 (ASCR), LC06040 (MŠMT), LC510 (MŠMT), and the Fellowship J. E. Purkyně (ASCR).

7. References

- Allen, M.; Hud, N.; Balooch, M.; Tench, R.; Siekhaus, W. & Balhorn, R. 1992. Tip-radius-induced artifacts in AFM images of protamine-complexed DNA fibers. *Ultramicroscopy*, 42-44: 1095-1100.
- Azulay, D.; Balberg, I.; Chu, V.; Conde, J. P. & Millo O. 2005. Current routes in hydrogenated microcrystalline silicon. *Physical review B* 71, 113304.
- Beard, J. D.; Gordeev, S. N. & Guy, R. H. 2011. AFM Nanotools for Surgery of Biological Cells. *Journal of Physics: Conference Series*: 012003.
- Bernardes-Filho, R. & Assis, O. B. G. de. 2005. Development of an algorithm for tip-related artifacts identification in AFM biological film imaging. *Brazilian Archives of Biology and Technology*, 48(4): 667-674.
- Calleja, M.; Nordström, M.; Alvarez, M.; Tamayo, J.; Lechuga, L. M. & Boisen, A. 2005. Highly sensitive polymer-based cantilever-sensors for DNA detection. *Ultramicroscopy*, 105(1-4): 215-222.
- Crampton, N.; Yokokawa, M.; Dryden, D. T.; Edwardson, J. M.; Rao, D. N.; Takeyasu, K.; Yoshimura S.H.; Henderson R.M. 2007. Fast-scan atomic force microscopy reveals that the type III restriction enzyme EcoP15I is capable of DNA translocation and looping. *Proceedings of the National Academy of Sciences*, 104(31): 12755.
- Darling, E. M. 2011. Force scanning: a rapid, high-resolution approach for spatial mechanical property mapping. *Nanotechnology*, 22(17): 175707.
- Diao, P.; Zhang, D, Guo, M. & Zhang Q. 2009. „Comments on ‘Electric-Field-Assisted Growth of Highly Uniform and Oriented Gold Nanotriangles on Conducting Glass Substrates’”. *Advanced Materials*, 21 (13): 1317-1319. doi:10.1002/adma.200801390.
- Dongmo, S. 1996. Blind restoration method of scanning tunneling and atomic force microscopy images. *Journal of Vacuum Science & Technology B: Microelectronics and Nanometer Structures*, 14(2): 1552.
- Eaton, P. 2010. *Atomic force microscopy*. Oxford; New York: Oxford University Press.
- Gainutdinov & Arutyunov. 2001. Artifacts in Atomic Force Microscopy, *Russian Microelectronics*, 30(4): 219-224.
- Garfias-García, E.; Romero-Romo, M.; Ramírez-Silva, M. T.; Morales, J. & Palomar-Pardavé, M. 2008. Mechanism and kinetics of the electrochemical formation of polypyrrole under forced convection conditions. *Journal of Electroanalytical Chemistry*, 613(1): 67-79.
- Ge, G.; Han, D.; Lin, D.; Chu, W.; Sun, Y.; Jiang, L.; Ma W.; Wang C. 2007. MAC mode atomic force microscopy studies of living samples, ranging from cells to fresh tissue. *Ultramicroscopy*, 107(4-5): 299-307.
- Giessibl, F. J. 2006. Higher-harmonic atomic force microscopy. *Surface and Interface Analysis*, 38(12-13): 1696-1701.

- Graham, H. K.; Hodson, N. W.; Hoyland, J. A.; Millward-Sadler, S. J.; Garrod, D.; Scothern, A. et al. 2010. Tissue section AFM: In situ ultrastructural imaging of native biomolecules. *Matrix Biology*, 29(4): 254-260.
- Hamon, L.; Pastré, D.; Dupaigne, P.; Breton, C. L.; Cam, E. L. & Piétrement, O. 2007. High-resolution AFM imaging of single-stranded DNA-binding (SSB) protein–DNA complexes. *Nucleic acids research*, 35(8): e58.
- Hawkes, P. 1988. *Advances in electronics and electron physics*. Boston: Academic Press.
- Helenius, J.; Heisenberg, C.-P.; Gaub, H. E. & Muller, D. J. 2008. Single-cell force spectroscopy. *Journal of Cell Science*, 121(11): 1785-1791.
- Hills, M. M. 1995. Carbon dioxide jet spray cleaning of molecular contaminants. *Journal of Vacuum Science & Technology A: Vacuum, Surfaces, and Films*, 13(1): 30.
- Hoffmann R.; Kriele A.; Obloh H.; Tokuda N.; Smirnov W.; Yang N. & Nebel C.E. 2011. The creation of a biomimetic interface between boron-doped diamond and immobilized proteins. *Biomaterials*, 32, 7325-7332.
- Hyde, M. E.; Jacobs, R. M. J. & Compton, R. G. 2004. An AFM Study of the Correlation of Lead Dioxide Electrocatalytic Activity with Observed Morphology. *The Journal of Physical Chemistry B*, 108(20): 6381-6390.
- Chapman, B. Glow discharge processes: Sputtering and Plasma Etching, *John Wiley & Sons*, New York (1980).
- Checco, A.; Cai, Y.; Gang, O. & Ocko, B. M. 2006. High resolution non-contact AFM imaging of liquids condensed onto chemically nanopatterned surfaces. *Ultramicroscopy*, 106, (8-9): 703-708.
- Chen, I.-C.; Chen, L.-H.; Orme, C. A. & Jin, S. 2007. Control of Curvature in Highly Compliant Probe Cantilevers during Carbon Nanotube Growth. *Nano Letters*, 7(10): 3035-3040.
- Chen, P.; Dong, H.; Chen, L.; Sun, Q. & Han, Dong. 2009. Application of atomic force microscopy to living samples from cells to fresh tissues. *Chinese Science Bulletin*, 54(14): 2410-2415.
- Chen, Y.; Cai, J.; Liu, M.; Zeng, G.; Feng, Q. & Chen, Z. 2004. Research on double-probe, double-and triple-tip effects during atomic force microscopy scanning. *Scanning*, 26(4): 155-161.
- Choi, I.; Kim, Y.; Kim, J. H.; Yang, Y. I.; Lee, J.; Lee, S.; Hong, S. & Yi, J. 2008. Fast image scanning method in liquid-AFM without image distortion. *Nanotechnology*, 19: 445701.
- Chong, K. F.; Loh, K. P.; Vedula, S. R. K.; Lim, C. T.; Sternschulte, H.; Steinmüller, D.; et al. 2007. Cell Adhesion Properties on Photochemically Functionalized Diamond. *Langmuir*, 23(10): 5615-5621.
- Keller, D. & Franke, F. 1993. Envelope reconstruction of probe microscope images. *Surface Science*, 294(3): 409-419.
- Kienberger, F.; Pastushenko, V. P.; Kada, G.; Puntheeranurak, T.; Chtcheglova, L.; Riethmueller, C.; Rankl, C.; Ebner & A.; Hinterdorfer, P. 2006. Improving the contrast of topographical AFM images by a simple averaging filter. *Ultramicroscopy*, 106(8-9): 822-828.
- Klinov, D. V.; Neretina, T. V.; Prokhorov, V. V.; Dobrynina, T. V.; Aldarov, K. G. & Demin, V. V. 2009. High-resolution atomic force microscopy of DNA. *Biochemistry (Moscow)*, 74(10): 1150-1154.

- Kozak, H.; Kromka, A.; Ledinsky, M. & Rezek, B. 2009. Enhancing nanocrystalline diamond surface conductivity by deposition temperature and chemical post-processing. *Phys. Stat. Sol. (a)* 206, 276–280.
- Kozak, H.; Remes, Z.; Kromka, A. & Ledinsky, M. 2011. Optical characterisation of organosilane-modified nanocrystalline diamond films. *Chemical Papers*, 65 (1): 36–41.
- Kransnoslobodtsev, A. V.; Shlyakhtenko, L. S.; Ukraintsev, E.; Zaikova, T. O.; Keana, J. F. W. & Lyubchenko, Y. L. 2005. Nanomedicine and protein misfolding diseases. *Nanomedicine: Nanotechnology, Biology and Medicine*, 1(4): 300–305.
- Kühle, A.; Sorensen, A. H.; Zandbergen, J. B. & Bohr, J. 1998. Contrast artifacts in tapping tip atomic force microscopy. *Applied Physics A: Materials Science & Processing*, 66(7): S329–S332.
- Kuznetsov, Y. G.; Victoria, J. G.; Robinson Jr, W. E. & McPherson, A. 2003. Atomic force microscopy investigation of human immunodeficiency virus (HIV) and HIV-infected lymphocytes. *Journal of virology*, 77(22): 11896.
- Kwon, E.-Y.; Kim, Y.-T. & Kim, D.-E. 2009. Investigation of penetration force of living cell using an atomic force microscope. *Journal of Mechanical Science and Technology*, 23(7): 1932–1938.
- Lambert, J.; Guthmann, C. & Saint-Jean, M. 2003. Relationship between charge distribution and its image by electrostatic force microscopy. *Journal of Applied Physics*, 93(9): 5369.
- LeDue, J. M.; Lopez-Ayon, M.; Burke, S. A.; Miyahara, Y. & Grütter, P. 2009. High Q optical fiber tips for NC-AFM in liquid. *Nanotechnology*, 20(26): 264018.
- Lin, S.-M. & Lin, C.-C. 2009. Phase shifts and energy dissipations of several modes of AFM: Minimizing topography and dissipation measurement errors. *Precision Engineering*, 33(4): 371–377.
- Lo, Y.-S.; Huefner, N. D.; Chan, W. S.; Dryden, P.; Hagenhoff, B. & Beebe, T. P. 1999. Organic and Inorganic Contamination on Commercial AFM Cantilevers. *Langmuir*, 15(19): 6522–6526.
- Maeda, Y.; Matsumoto, T. & Kawai, T. 1999. Observation of single-and double-stranded DNA using non-contact atomic force microscopy. *Applied surface science*, 140(3–4): 400–405.
- Mahmood, I. A. & Moheimani, S. O. R. 2009. Making a commercial atomic force microscope more accurate and faster using positive position feedback control. *Review of Scientific Instruments*, 80(6): 063705.
- Shimizu N.; Ikeda M.; Yoshida E.; Murakami H.; Miyazaki S. & Hirose M. 2000. Charging states of Si quantum dots as detected by AFM/Kelvin probe technique. *Jpn. J. Appl. Phys.*, 39, 2318–2320.
- Moreno-Herrero, F.; Colchero, J.; Gómez-Herrero, J. & Baró, A. 2004. Atomic force microscopy contact, tapping, and jumping modes for imaging biological samples in liquids. *Physical Review E*, 69(3).
<http://link.aps.org/doi/10.1103/PhysRevE.69.031915>, 2011.
- Morton, D. N.; Roberts, C. J.; Hey, M. J.; Mitchell, J. R.; Hipkiss, J. & Vercauteren, J. 2003. Surface Characterization of Caramel at the Micrometer Scale. *Journal of Food Science*, 68(4): 1411–1415.

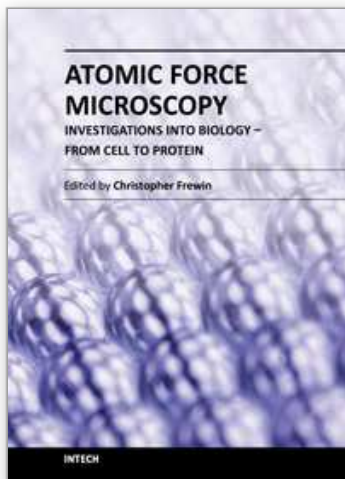
- Müller, D. J.; Helenius, Jonne, Alsteens, D. & Dufrêne, Y. F. 2009. Force probing surfaces of living cells to molecular resolution. *Nature Chemical Biology*, 5(6): 383-390.
- Naik, T. 2003. Dynamic response of a cantilever in liquid near a solid wall. *Sensors and Actuators A: Physical*, 102(3): 240-254.
- Nie, H.-Y. & McIntyre, N. S. 2007. Unstable amplitude and noisy image induced by tip contamination in dynamic force mode atomic force microscopy. *Review of Scientific Instruments*, 78(2): 023701.
- Rasool, H. I.; Wilkinson, P. R.; Stieg, A. Z. & Gimzewski, J. K. 2010. A low noise all-fiber interferometer for high resolution frequency modulated atomic force microscopy imaging in liquids. *Review of Scientific Instruments*, 81(2): 023703.
- Reed, J.; Schmit, J.; Han, S.; Wilkinson, P. & Gimzewski, J. 2009. Interferometric profiling of microcantilevers in liquid. *Optics and Lasers in Engineering*, 47(2): 217-222.
- Rezek, B.; Shin, D.; Nakamura, T. & Nebel, C. E. 2006. Geometric Properties of Covalently Bonded DNA on Single-Crystalline Diamond. *Journal of the American Chemical Society*, 128: 3884-3885.
- Rezek, B.; Nebel, C.E. 2006. Electronic properties of plasma hydrogenated diamond surfaces: a microscopic study. *Diamond Relat. Mater.* 15, 1374 – 1377.
- Rezek, B., Shin, D. & Nebel, C. E. 2007. Properties of hybridized DNA arrays on single-crystalline undoped and boron-doped (100) diamonds studied by atomic force microscopy in electrolytes. *Langmuir* 23(14): 7626-7633.
- Rezek, B.; Shin, D.; Uetsuka, H. & Nebel, C. E. 2007. Microscopic diagnostics of DNA molecules on mono-crystalline diamond. *Physica status solidi (a)*, 204(9): 2888-2897.
- Rezek, B.; Ukraintsev, E.; Michalíková, L.; Kromka, A.; Zemek, J. & Kalbacova, M. 2009. Adsorption of fetal bovine serum on H/O-terminated diamond studied by atomic force microscopy. *Diamond and Related Materials*, 18(5-8): 918-922.
- Rezek, B.; Ukraintsev, E.; Kromka, A.; Ledinský, M.; Brož, A.; Nosková, L.; Hartmannova, H. & Kalbacova, M. 2010. Assembly of osteoblastic cell micro-arrays on diamond guided by protein pre-adsorption. *Diamond and Related Materials*, 19(2-3): 153-157.
- Rezek, B.; Krátká, M.; Ukraintsev, E.; Babchenko, O.; Kromka, A.; Brož, A.; Kalbacova M. Diamond as functional material for bioelectronics and biotechnology In: "New Perspectives in Biosensors Technology and Applications" Intech 2011, pp. 177-196, ISBN 978-953-307-448-1.
- Rezek, B.; Ukraintsev, E. & Kromka, A. 2011. Optimizing atomic force microscopy for characterization of diamond-protein interfaces. *Nanoscale research letters*, 6(1): 1-10.
- Ricci, D. & Braga, P. C. 2003. Recognizing and Avoiding Artifacts in AFM Imaging. *Atomic Force Microscopy*: 25-38.
<http://www.springerlink.com/openurl.asp?genre=book&id=doi:10.1385/1-59259-647-9:25>, 2011, New Jersey: Humana Press.
- Sahin, O.; Quate, C.; Solgaard, O. & Atalar, A. 2004. Resonant harmonic response in tapping-mode atomic force microscopy. *Physical Review B*, 69(16).
<http://link.aps.org/doi/10.1103/PhysRevB.69.165416>, 2011.
- Sajanlal, P. R. & Pradeep, T. 2008. Electric-Field-Assisted Growth of Highly Uniform and Oriented Gold Nanotriangles on Conducting Glass Substrates. *Advanced Materials*, 20(5): 980-983.

- Shekhawat, G. S.; Lambert, M. P.; Sharma, S.; Velasco, P. T.; Viola, K. L.; Klein, W. L. & Dravid V.P. 2009. Soluble state high resolution atomic force microscopy study of Alzheimer's β -amyloid oligomers. *Applied Physics Letters*, 95(18): 183701.
- Sokolov, I. 2007. Atomic force microscopy in cancer cell research. *Cancer Nanotechnology*. Valencia, CA: American Scientific Publishers, 1-17.
- Solares, S. D. 2007. Frequency and force modulation atomic force microscopy: low-impact tapping-mode imaging without bistability. *Measurement Science and Technology*, 18: L9.
- Sotres, J.; Lostao, A.; Gomezmoreno, C. & Baro, A. 2007. Jumping mode AFM imaging of biomolecules in the repulsive electrical double layer. *Ultramicroscopy*, 107(12): 1207-1212.
- Su, F.; Wei, J. & Liu, Y. 2005. Removal of AFM moiré measurement errors due to non-linear scan and creep of probe. *Nanotechnology*, 16: 1681.
- Thormann, E.; Pettersson, T. & Claesson, P. M. 2009. How to measure forces with atomic force microscopy without significant influence from nonlinear optical lever sensitivity. *Review of Scientific Instruments*, 80(9): 093701.
- Thundat, T.; Zheng, X.-Y.; Chen, G. Y.; Sharp, S. L.; Warmack, R. J. & Schowalter, L. J. 1993. Characterization of atomic force microscope tips by adhesion force measurements. *Applied Physics Letters*, 63(15): 2150.
- Touhami, A.; Jericho, M. H. & Beveridge, T. J. 2004. Atomic force microscopy of cell growth and division in *Staphylococcus aureus*. *Journal of bacteriology*, 186(11): 3286.
- Ukrainitsev, E. V.; Kiselev, G. A.; Kudrinskii, A. A.; Lisichkin, G. V. & Yaminskii, I. V. 2007. Formation of lysozyme fibrils on a solid support. *Polymer Science Series B*, 49(1-2): 6-9.
- Ukrainitsev, E.; Rezek, B.; Kromka, A.; Broz, A. & Kalbacova, M. 2009. Long-term adsorption of fetal bovine serum on H/O-terminated diamond studied *in situ* by atomic force microscopy. *physica status solidi (b)*, 246(11-12): 2832-2835.
- Velegol, S. B.; Pardi, S.; Li, X.; Velegol, D. & Logan, B. E. 2003. AFM Imaging Artifacts due to Bacterial Cell Height and AFM Tip Geometry. *Langmuir*, 19(3): 851-857.
- Verveniotis, E.; Kromka, A.; Ledinský, M.; Čermák, J. & Rezek, B. 2011. Guided assembly of nanoparticles on electrostatically charged nanocrystalline diamond thin films. *Nanoscale Research Letters*, 6: 144.
- Vetushka, A.; Fejfar, A.; Ledinský, M.; Rezek, B.; Stuchlík, J. & Kočka J. 2010. Comment on "Current routes in hydrogenated microcrystalline silicon". *Physical review B* 81, 237301.
- Volle, C. B.; Ferguson, M. A.; Aidala, K. E.; Spain, E. M. & Núñez, M. E. 2008. Quantitative Changes in the Elasticity and Adhesive Properties of *Escherichia coli* ZK1056 Prey Cells During Predation by *Bdellovibrio bacteriovorus* 109J. *Langmuir*, 24(15): 8102-8110.
- Wadu-Mesthrige, K.; Amro, N. A.; Garno, J. C.; Cruchon-Dupeyrat, S. & Liu, G. Y. 2001. Contact resonance imaging—a simple approach to improve the resolution of AFM for biological and polymeric materials. *Applied surface science*, 175: 391-398.
- Wu, Y.; Hu, Y.; Cai, J.; Ma, S.; Wang, X. & Chen, Y. 2008. The analysis of morphological distortion during AFM study of cells. *Scanning*, 30(5): 426-432.
- You, H. 2000. Atomic force microscopy imaging of living cells: a preliminary study of the disruptive effect of the cantilever tip on cell morphology. *Ultramicroscopy*, 82(1-4): 297-305.

- You, H. X. & Yu, L. 1999. Atomic force microscopy imaging of living cells: progress, problems and prospects. *Methods in cell science*, 21(1): 1-17.
- Zhao, M.; Sharma, V.; Wei, H.; Birge, R. R.; Stuart, J. A.; Papadimitrakopoulos, F. & Huey B.D. 2008. Ultrasharp and high aspect ratio carbon nanotube atomic force microscopy probes for enhanced surface potential imaging. *Nanotechnology*, 19(23): 235704.

IntechOpen

IntechOpen



Atomic Force Microscopy Investigations into Biology - From Cell to Protein

Edited by Dr. Christopher Frewin

ISBN 978-953-51-0114-7

Hard cover, 354 pages

Publisher InTech

Published online 07, March, 2012

Published in print edition March, 2012

The atomic force microscope (AFM) has become one of the leading nanoscale measurement techniques for materials science since its creation in the 1980's, but has been gaining popularity in a seemingly unrelated field of science: biology. The AFM naturally lends itself to investigating the topological surfaces of biological objects, from whole cells to protein particulates, and can also be used to determine physical properties such as Young's modulus, stiffness, molecular bond strength, surface friction, and many more. One of the most important reasons for the rise of biological AFM is that you can measure materials within a physiologically relevant environment (i.e. liquids). This book is a collection of works beginning with an introduction to the AFM along with techniques and methods of sample preparation. Then the book displays current research covering subjects ranging from nano-particulates, proteins, DNA, viruses, cellular structures, and the characterization of living cells.

How to reference

In order to correctly reference this scholarly work, feel free to copy and paste the following:

E. Ukraintsev, A. Kromka, H. Kozak, Z. Remeš and B. Rezek (2012). Artifacts in Atomic Force Microscopy of Biological Samples, Atomic Force Microscopy Investigations into Biology - From Cell to Protein, Dr. Christopher Frewin (Ed.), ISBN: 978-953-51-0114-7, InTech, Available from: <http://www.intechopen.com/books/atomic-force-microscopy-investigations-into-biology-from-cell-to-protein/artifacts-in-atomic-force-microscopy-of-biological-samples>

INTech
open science | open minds

InTech Europe

University Campus STeP Ri
Slavka Krautzeka 83/A
51000 Rijeka, Croatia
Phone: +385 (51) 770 447
Fax: +385 (51) 686 166
www.intechopen.com

InTech China

Unit 405, Office Block, Hotel Equatorial Shanghai
No.65, Yan An Road (West), Shanghai, 200040, China
中国上海市延安西路65号上海国际贵都大饭店办公楼405单元
Phone: +86-21-62489820
Fax: +86-21-62489821

© 2012 The Author(s). Licensee IntechOpen. This is an open access article distributed under the terms of the [Creative Commons Attribution 3.0 License](#), which permits unrestricted use, distribution, and reproduction in any medium, provided the original work is properly cited.

IntechOpen

IntechOpen